Analysis of field Distribution and Characteristic Performance of Induction Motor with Faults by Using Finite Element Method

Dr. Khaleel J. Hammadi

Lecturer, Electronic and Electronic Techniques- Baghdad, Ministry of High Education and Scientific Research, Iraq

Abstract: The basic methods of diagnosis broken rotor bars is presented in this paper. The time stepping in finite elements techniques is used and investigated in details. Widely comparison of introduced methods with another techniques shows that the suggested technique provides fast and accurate path to diagnosis the faults earlier which consider efficient way to reduce the faults in induction motors by mean of time different of torque in healthy and faulty motors and stator current waveforms. Additionally, the flux distribution is considered as the third techniques in this study. A result shows the fast extraction of faults in the induction motors and new developing techniques is founded.

Keywords: squirrel cage, induction motor, healthy and faulty motor, FEM.

I. INTRODUCTION

Induction motors are still widely used drive in industry; there are many techniques and products on analysis of the motor and its optimal use. In spite of such products, industry is confronted with unexpected faults and lifetime reduction of the motors. Meanwhile, by enhancement of the power of the motor rating, monitoring tools loss their economic justification. Therefore, achieving a more advanced and precise technology is required for fault diagnosis [1, 2]. Asymmetry of stator and rotor increases the stator harmonics current, torque variations, temperature rise; mean torque decreases and losses increase which leads to a lower efficiency. These signs and some of their secondary signs can be used as indexes for fault diagnosis of the motor. So far, for detection of these indexes, various methods have been proposed which cover different aspects of science and technology [3]. Deviation of magnetic potential vector and asymmetrical magnetic flux distribution has been used to diagnose the broken rotor bars [4]. The drawback of this method is fixing its sensor within the air gap and effect of the disturbance and noise on the sent signal. Gyration radius may be employed to detect the rotor bars breakage [5, 6]. This is an invasive diagnosis method and needs costly measurement equipment. In [7], an asymmetrical magnetic flux distribution, torque and speed fluctuation has been used to diagnose the rotor broken bars in startup mode. In [8], effect of the load magnitude upon the faults is studied. In [9], pattern recognition and k-nearest neighbors rule has been used to diagnose the rotor broken bars.

In [10, 11], a harmonic component in the stator current caused by the fault has been used to diagnose the broken rotor bars. In [12] an inverter-fed induction motor with broken bars has been investigated and shown that the fundamental frequency component is varying and the existing side harmonic frequency components $(1 \pm 2s)f_s$

vary and fault diagnosis by this frequency harmonics is difficult. In [13,14] , instantaneous power frequency spectrum has been considered and shown that the existing peaks in power frequency spectrum related to the frequency of the fault and is independent of the poles number. Finite element method (FEM) is used here to model broken rotor bars in an induction motor. In this modeling, geometrical and physical characteristics of all parts of the motor, spatial distribution of stator windings, slots on both sides of the air gap. Also the current of the broken bar is taken to be zero, instead resistance of the broken bar is considered large enough. So far, numbers of broken bars and varying load have been considered in the literature for diagnosis and analysis of the rotor bars break [15].

Table I. specification of suggested motor

Poles numbers	4
Total phase number	3
Stator external width	160 mm
Stator internal width	68mm
Width of Air gap	1mm
length of axial	40mm
stator slots	30
rotor bars	24
volte	400
frequency	50
stator turns	180

II. CONCEPT OF BROKEN BAR

Some of the more common secondary effects of broken rotor bars are:
- If one or more rotor bars are broken, the healthy bars are forced to carry additional current leading to rotor core

damage from persistent elevated temperatures in the vicinity of the broken bars and current passing through the core from broken to healthy bars.

• Broken bars cause torque and speed oscillations in the rotor, provoking premature wear of bearings and other driven components.

• Large air pockets in die-cast aluminium alloy rotor windings can cause no uniform bar expansion leading to rotor bending and imbalance that causes high vibration levels from premature bearing wear.

• As the rotor rotates at high radial speed, broken rotor bars can lift out of the slot due to centrifugal force and strike against the stator winding causing a catastrophic motor failure.

e) Rotor asymmetry (the rotor rotating off-centre), both static and dynamic, could cause the rotor to rub against the stator winding leading to rotor core damage and even a catastrophic fault.

III. FEM OF THE INDUCTION MOTOR

Generally, there are three major methods for modeling, analysis and diagnosis of faults in induction motor, winding function method (WFM), equivalent magnetic circuit method (MECM) and finite element method (FEM). Induction motor is a highly symmetrical electromagnetic system. Any fault will induce a certain degree of asymmetry.
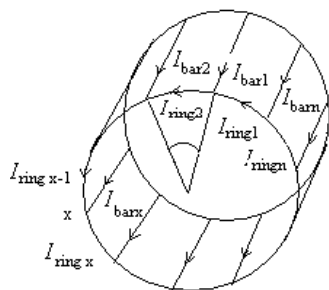

Fig.1 allocation structure

Broken rotor bars in induction motors can cause asymmetry in the resistances of rotor phases Figure 1. Which results in asymmetry of the rotating electromagnetic field in the air gap between the motor stator and rotor? In turn, this will eventually induce frequency harmonics in the stator current. Therefore, in the mathematical model, an additional resistance is added into each of the rotor phases to simulate broken rotor bar faults (16).

$$\Delta r_{ra,b,c} = \frac{3n_{bb}}{N_b - 3n_{bb}} r_r \qquad (1)$$

where $\Delta r_{ra,b,c}$ rotor resistance changes in phase a, b and c, respectively, due to broken bar faults, and n_{bb} and N_b are reminded as the number of broken and the total rotor bars, respectively defined as (17).

The function of rotor resistance change $\Delta r_{ra,b,c}$ due to rotor defects is derived based on the assumption that the broken bars are contiguous, neither the end ring resistance nor the magnetizing current are taken account. The rotor phase equivalent resistance of a healthy induction motor is given as (18).

$$r_r = \frac{(2N_S)^2}{N_b/3} \left[r_b + \frac{2}{N_b(2\sin\frac{\alpha}{2})^2} r_e \right] \qquad (2)$$

where r_b and r_e represent the rotor bar and end-ring resistances, respectively, and N_s is the equivalent stator winding turns. As in the assumptions, when r_e is neglected, r_r then simplifies to;

$$r_r \approx \frac{(2N_S)^2}{N_b/3} r_b \qquad (3)$$

Then, the resistance of one phase rotor with n_{bb} contiguous broken rotor bars becomes

$$r^*_r \approx \frac{(2N_S)^2}{\frac{N_b}{3} - n_{bb}} r_b \qquad (4)$$

and the increment Δ_r is obtained as

$$\Delta_r = r^*_r - r_r = \frac{3n_{bb}}{N_b - 3n_{bb}} r_r \qquad (5)$$

$$\Delta I = f(\Delta_r) \qquad (6)$$

The second quantitative fault evaluation equation is proposed by (19) as;

$$\frac{I_{bb}}{I} = \frac{\sin\alpha}{P(2\pi - \alpha)} \qquad (7)$$

where I_{bb} and I are the amplitudes of the sideband and the fundamental frequencies in the stator current spectrum, respectively, P is the number of motor poles, α is the electrical angle of a contiguous group of broken rotor bars, given by;

$$\alpha = \frac{\pi P n_{bb}}{N_b} \qquad (8)$$

When the motor loads, and consequently the rotor speed, are not constant, I_{bb} should be replaced by the sum of the amplitudes of the two sideband frequencies $(1 \pm 2s)f_s$.

V. SIMULATION RESULTS

The foundations of a technique for diagnosis and characterization of effects broken rotor bars in 3-phase squirrel-cage induction motors based on the FEM approach. These studies are performed by using the model to compute healthy case and broken rotor bars fault performance data, which contains stator current waveforms, air-gap flux density and the distribution of magnetic field. From this data, the faulty signatures are extracted. In this section, the results of the induction motor simulation for the cases of healthy rotor and faulty broken rotor bars are presented.

Simulation and modeling the changes in electromagnetic characteristics of 3-phase squirrel-cage induction motor due to any fault can be easily observed without the need of destroying a motor, or experimenting in laboratories motors with different fault types. This work provides an adequate proof of concept and insight about MCSA in fault detection and monitoring for 3-phase squirrel- cage induction motor

by using finite element opera-2d. Under the rated load conditions, the distribution of magnetic field for the case of no broken bars is symmetrical, while the symmetry of magnetic field distribution is distorted in the case of broken bars, and a higher degree of magnetic saturation can be observed in rotor teeth around the broken bar area as a result of the lack of local demagnetization slip frequency-induced current in these rotor slots, which might result in a degradation in the mechanical performance of the induction motor. Samples of flux plots for the motor under rated load condition for the cases of symmetrical and asymmetrical rotor condition are shown in Figure 2.

That in the case of the faulty motor the magnetic flux density B in the air gap is more unbalanced and it has a pronounced fluctuation, due to the backward rotating magnetic field produced due to rotor faults Figure 4. This is rotating at the slip speed, $n_2 = n_1(2s - 1)$, with respect to the stator [20].
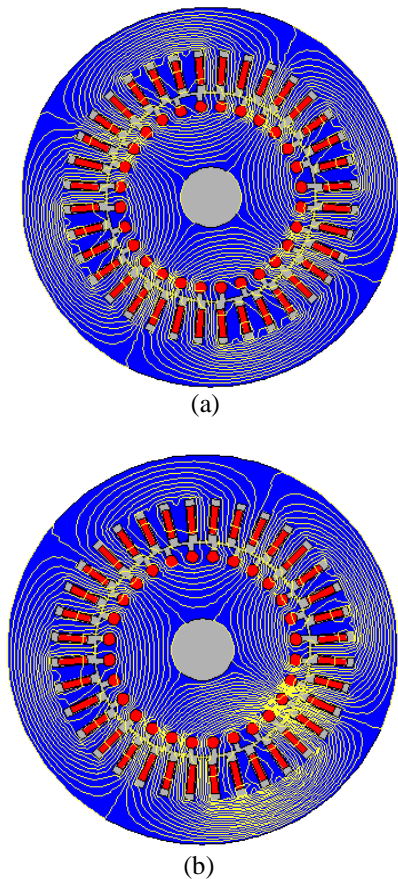
Therefore, by increasing the number of broken rotor bars in the motor, a higher asymmetry of the flux distribution occurs. By increasing the amplitude of the harmonic components in the flux waves due to the fault the amplitude of the harmonic frequency components in the stator current are also risen due to fault.
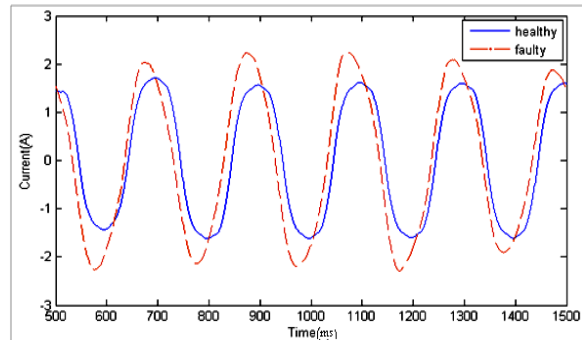

Fig.3. Current stator in healthy and faulty state condition

Meanwhile, samples of air-gap radial flux density waveforms for the cases of symmetrical and asymmetrical rotor conditions are given in Figure 4. From this figure, it can be observed that the air-gap radial flux density waveform of faulty motor is pronouncedly more asymmetrical than that in healthy motor. This asymmetry is a direct result of the broken bars in the rotor. In addition, this asymmetry in the radial flux density under rotor fault condition can result in a non-uniform distribution of induced slip frequency currents in the rotor bars.

Furthermore, notice the higher magnitude of the air gap radial flux density waveform under rotor asymmetrical condition, this can degrade the performance characteristics, such as the developed torque of the motor.
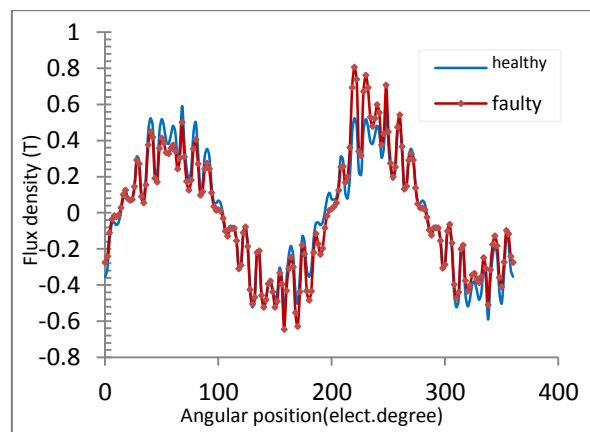

(a)

(b)

Fig.2. (a) healthy motor (b) faulty motor

Fig.4. Magnetic flux B in the air gap healthy and faulty motor

The simulated stator current waveforms by using FEM opera-2d for the case of broken rotor bars is given in Figure 3. One can notice that the amplitude of stator current changes significantly compared to that in the healthy cage. The reason is that the broken rotor bars causes asymmetry of flux distribution which leads to higher harmonics in the faulty motor. Broken rotor bars produce certain frequencies in the flux waveform and the rotating flux waves can induce the currents with the same frequency in the stator current.

The magnetic torque ripples are also increased in case of the faulty induction motor than in case of the motor without any rotor fault. Figure 5 presents the time variations of torque for a healthy and faulty induction motor with two broken rotor bars. Comparison of healthy and faulty state indicates that the rotor broken bars increases the oscillation of the developed torque. One can easily notice that in the

case of the motor having broken rotor bars the torque has the highest value. One can also notice the time variation of torque profile increases in faulty state comparison with healthy state i.e. higher torque ripples in induction motor having broken rotor bars. This is due to the fact that under broken rotor bar condition and load, the non-zero backward-rotating field interacts with the rotor currents to produce a torque variation at twice the slip frequency. This torque is then superimposed on the torque produced by the forward-rotating field resulting in the modulating effect of the steady-state developed torque.
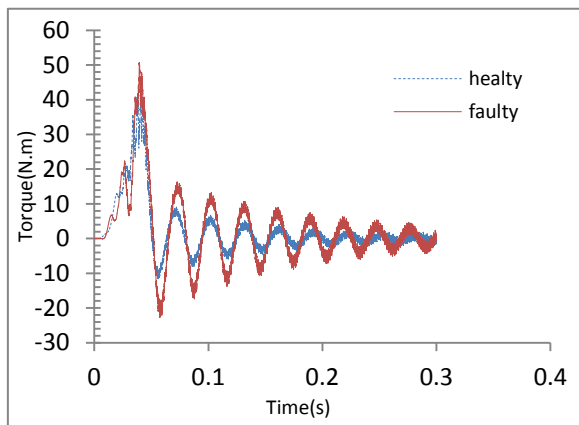

Fig.5. Time difference of torque

VI. CONCLUSION

Finite element method was used to determine the magnetic field distribution both in healthy induction machine and the machine having three broken rotor bars. The presented FEM analysis is one effective and inexpensive method for studying the influence of rotor faults on behavior of three phase squirrel-cage induction machines. This method also allows studying the effect of rotor faults on stator line currents, applicable on developing effective fault diagnostic tools. Once again it has been proved that the bars next to broken ones are the most exposed to future damage, due to the very high value bar currents.

REFERENCES

[1] Nandi S, Bharadwaj R, Tolivat HA, Parlos AG. Study of three phase induction motors with in cipient rotor cage faults under different supply conditions, In; proceedings of the IEEE-IAS 1999 annual meeting, vol.3.

[2] J. Faiz, B.M. Ebrahimi and M.B.B. Sharifian, Different faults and their diagnosis techniques in three phase squirrel-cage induction motors – a review, J Electromag 26 (2006).

[3] G.L. Paoletti and A. Rose, Improving existing motor protection for medium voltage motors, IEEE Trans Ind Appl 25 (3) (1989).

[4] R. Fiser, Application of a finite element method to predict damage induction motor performance, IEEE Trans Magn 37 (5) (2001).

[5] R.J. Povinelli, J.F. Bangura, N.A.O. Demerdash and R.H. Brown, Diagnostics of bar and end-ring connector breakage faults in poly phase induction motors through a novel dual track of time-series data mining and time-stepping coupled FE – state space modeling, IEEE Trans Energy Convers 17 (1) (2002).

[6] J.F. Bangura, R.J. Povinelli, N.A.O. Demerdash and R.H. Brown, Diagnostics of eccentricities and bar/end-ring connector breakages

in poly phase induction motors through a combination of time series data mining and time-stepping coupled FE – state space techniques Industry Applications, IEEE Trans Ind Appl 39 (4) (2003).

[7] J. Faiz, B.M. Ebrahimi and M.B.B. Sharifian, Time stepping finite element analysis of rotor broken bars fault in a three-phase squirrel-cage induction motor, Progr Electromag Res PIER 68 (2007).

[8] B. Mirafzal and N.A.O. Demerdash, Effects of load magnitude on diagnosis broken bar faults in induction motors using the pendulous oscillation of the rotor magnetic field orientation, IEEE Trans Ind Appl 41 (3) (2005).

[9] O. Ondel, E. Boutleux and G. Clerc, A method to detect broken bars in induction machine pattern recognition techniques, IEEE Trans Ind Appl 42 (4) (2006).

[10] M. Haji and H.A. Toliyat, Pattern recognition – a technique for induction machines rotor broken bar detection, IEEE Trans Energy Convers 16 (4) (2001).

[11] J.F. Bangura and N.A. Demerdash, Diagnosis and characterization of effects of broken bars and connectors in squirrel-cage induction motors by a time-stepping coupled finite element – state space modeling approach, IEEE Trans Energy Convers 14 (4) (1999).

[12] A.G. Innes and R.A. Langman, the detection of broken rotor bars in variable speed induction motor drives, ICEM94 (1994).

[13] S.F. Legowski and A.M. Trzynadlowski, Instantaneous stator power as a medium for the signature analysis of induction motors, IEEE IAS 95 (1995).

[14] Trzynadlowski AM, Ghasezadeh M, Legowski SF. Diagnostics of mechanical abnormalities in induction motors using instantaneous electric power. IEEE 1997; MBI 9.1–9.3.

[15] S.C. Ho, C.G. Hong and G.J. Hwang, Transient and steady state performance of a squirrel-cage induction motor, IEEE Proc Part B 136 (3) (1989).

[16] A. Bentounsi and A. Nicolas, "On line diagnosis of defaults on squirrel cage motor using FEM," IEEE Trans. Magn., vol. 34, no. 3, pp. 3511–3514, May 1998.

[17] FIŠER, R., MAKUC, D., AMBROŽIČ, V.: Evaluation of the induction motor cage fault stage using finite element method. Record of IEEE SDEMPED'2001, The 2001 IEEE International Symposium on Diagnostics for Electrical Machines, Power Electronics and Drives, Grado (Italy), pp. 627-631.

[18] Charles I. Hubert P. E, Prentice Hall, Electric machines, theory, operation, applications, adjustment, and control, second edition, TK2182. H83 2002.

[19] Theodore wildi, Electrical machines, drives, and power systems, fourth systems, Tk2182. W53 2000.

[20] Stephen J. Chapman British Aerospace Australia, Electric Machinery Fundamentals, Third Edition, MCGRAW-HILL.

[21] Tata McGraw-Hill, ELECTRIC MACHINES, Third Edition, Publishing Company Limited (NEW DELHI), Third reprint 2005 RYLQCRABRCAQZ.

[22] Juha Pyrhonen, Tapani Jokinen, Valeria Hrabovcova, Johu Wiley & Sons, Design of rotating electrical machines, Ltd TK2331.P97 2009,

[23] Workshop in Design and modeling of electrical machine, school of electrical & electronic engineering USM Engineering campus March-2009 By Engr. DR. Dahaman isahak.

BIOGRAPHY

Dr. Khaleel J. Hammadi has been a full-time lecturer in the college of Electronic and electronic Techniques-Baghdad, Ministry of high education and scientific research/Iraq. Received his MS and PhD Degree in Electrical engineering from University of Belgrade/ Yugoslavia /1984 and University since Malaysia –Malaysia /2011 respectively.